International Journal of Mechanical Sciences 110 (2016) 41–52

Contents lists available at ScienceDirect

International Journal of Mechanical Sciences

journal homepage: www.elsevier.com/locate/ijmecsci

Structural changes assessment in axial stressed beams through frequencies variation

T.-T.-H. Le [a], N. Point [a], P. Argoul [a,b], G. Cumunel [a,*]

[a] University Paris-Est, Laboratoire NAVIER (UMR 8205 CNRS-ENPC-IFSTTAR), Ecole des Ponts ParisTech, 6 et 8 Avenue Blaise Pascal, 77455 Marne-la-Vallée, France

[b] University Paris-Est, IFSTTAR (MAST/SDOA), 14-20 Boulevard Newton Champs-sur-Marne, F-77447 Marne-la-Vallée 2, France

ARTICLE INFO

Article history:
Received 1 July 2015
Received in revised form
2 February 2016
Accepted 13 February 2016
Available online 18 February 2016

Keywords:
Structural health monitoring
Modal analysis
Damage detection
Localization of notches
Euler–Bernoulli beam
Axial stressed beam

ABSTRACT

This paper concerns the localization and quantification of simultaneous structural modifications by dynamic analysis in Euler–Bernoulli beams, with or without axial force. A first-order estimation of frequency relative variation is derived from the continuous formulation. In case of localized variations of density and bending stiffness, this relation is a linear function of the relative variations of axial force, density, and bending stiffness, with nonlinear coefficients depending on the location of density and bending stiffness modification. These coefficients depend on the mode shapes of the initial state and not on the modes shapes of the modified beam. Taking advantage of the necessary compatibility of the estimations obtained for each frequency variation, a criterion is proposed to localize the modification. Once the location is determined, the coefficients of the linear system can be calculated and then the quantification of the relative variations is obtained. This localization and quantification procedure is then applied successfully to numerical simulations with simultaneous modifications of axial force, density, and bending stiffness. For validation, the method is applied to experimental data concerning beams without axial force and with mass modification or bending stiffness only. The results for the bending stiffness modification are discussed and compared to those obtained in literature.

© 2016 Elsevier Ltd. All rights reserved.

1. Introduction

The demand for enhanced performance and reliability of structures in terms of safety, noise-level and durability is ever increasing. Over the past few decades significant research has been conducted on structural health monitoring using many different techniques applied in various fields like aeronautics [1], industry [2] or civil engineering [3].

Given boundary conditions, a linear dynamic system can be defined either by its physical parameters (density, stiffness and damping) or by its modal parameters (eigenfrequencies, mode shapes, and modal damping ratios). Structural parameter modifications result in a change in modal parameters. This observation that changes in structural properties induce changes in modal parameters is the key to using modal methods for damage identification and structural health monitoring [4,5]. Among the great number of such techniques, we only cite some of the most recent reviews and papers [6–8]. The first step to use modal methods for damage detection is to estimate the modal parameters. Numerous approaches have been reported in Heylen [9], Maia [10], and Ewins [11]. Modal parameters estimation is therefore a necessary and initial tool, however, this is not the purpose of this article.

Beams are traditionally used to model buildings, civil engineering structural elements, and smaller structures such as frames of trucks, automobiles, lattice structures or machines. Moreover, as tension is of interest for cables (suspension bridge cables for example) or prestressed beams, our study is generalized to the transverse deflection of an Euler–Bernoulli beam with axial force. The question of localizing damages on a rod (axially loaded) or on a beam (loaded perpendicular to the neutral axis) has been extensively studied in literature especially in the case of a beam without axial force [12–14].

A cracked beam is often modeled by two segments connected by a rotational massless linear elastic spring [15,16], the equivalent stiffness of which is often obtained from fracture mechanics [17]. Considering appropriate compatibility requirements at the cracked section and the corresponding boundary conditions, analytical expressions for the characteristic equation of the beam are reached. Different problems can then be addressed like crack identification in a cantilever beam when clamp rigidity is unknown or changing [18], crack identification in uniform Timoshenko beams with an

* Corresponding author.
E-mail addresses: thi-thu-ha.le@eleves.enpc.fr (T.-T. Le), nelly.point@enpc.fr (N. Point), pierre.argoul@ifsttar.fr (P. Argoul), gwendal.cumunel@enpc.fr (G. Cumunel).

http://dx.doi.org/10.1016/j.ijmecsci.2016.02.008
0020-7403/© 2016 Elsevier Ltd. All rights reserved.

open edge crack [19], or analytical estimation extension based on Rayleigh's method for a beam having one or two cracks to find analytically natural frequencies and mode shapes in order to overcome weakness of solving eigenvalue problem [20]. To localize and evaluate the change of the bending stiffness, Morassi [21] has also proposed a method using generalized Fourier coefficients to calculate eigenfrequency sensitivity to the stiffness variation caused by the damage. He found from some generalized Fourier coefficients that frequency shifts contain information on the stiffness variation due to damage. Many researchers have also used a sensitivity method based on the eigenvalue equation, however most of them use a discrete form with mass and stiffness matrices [22,23]. Esfandiari [23] characterized the sensitivity of natural frequencies, in discrete form, as a second order function of the stiffness reduction. The main advantage of this method is that it does not require mode shapes of the damaged structure but only the frequencies.

Among the methods developed in the articles cited above, only a few frequencies, at least two [24] or three [18,25], can be used to detect and, sometimes, quantify the damage. However, the changes in mass and in the axial force are not taken into account. The change in mass is often supposed to be negligible compared to the stiffness variation. At the authors knowledge, few articles treat the case of beam with constant axial force [26,27] but the case of simultaneous variations of axial force, bending stiffness and density is not treated.

The technique proposed in this article belong to the class of vibration-based methods to detect and identify structural changes. The objectives of this paper are to establish an accurate relationship between structural properties and modal parameters for Euler–Bernoulli beams, and to develop a method to detect, localize and quantify simultaneous modifications. For that purpose, we start establishing from the continuous formulation of the eigenvalue equation, a first-order general estimate of the relative variation of each frequency as a function of the simultaneous variations of different mechanical parameters of the beam such as axial force, local density and local bending stiffness. This relationship can be used in two different ways. On one hand, measurements of the variations in modal properties can be used to detect and localize modifications in the structure, in time and space. And on the other hand, natural frequencies can be controlled by an appropriate modification of the structural parameters such as local mass or local stiffness.

In case of localized modifications of density and bending stiffness, the frequency relative variation leads to a linear function depending on the relative variations of axial force, density, and bending stiffness, with nonlinear coefficients depending on the location of density and bending stiffness modification. These nonlinear coefficients involve initial, or "healthy", mode shape and its first two derivatives of the corresponding frequency. A criterion is proposed to localize the modification by a minimization procedure, taking advantage of the necessary compatibility of the relations obtained for each frequency relative variation. For three modifications, at least three frequencies are needed and the reliability of this procedure increases with the number of available measured frequencies. Once the modifications are located, the coefficients of the linear system can be obtained. Then the linear system is solved via a linear least squares method in order to assess the quantification of the relative variations.

Our method requires p frequencies of the initial beam and the corresponding p frequencies of the modified beam (with p at least greater or equal to the number of simultaneous varying parameters). Our method does not require the mode shapes of the modified structure but only the mode shapes of the initial (or "healthy", undamaged, unmodified) beam. As in most practical cases, this initial state corresponds to a homogeneous, uniform beam, and knowing the type of boundary conditions it is possible to know theoretically, or to calculate numerically the modes shapes of the initial structure and their first two derivatives.

The article is organized as follows. The following section is devoted to the presentation of the proposed method for the identification of simultaneous modifications in Euler–Bernoulli beams. Relations between frequencies and normal modes for different boundary conditions of an Euler–Bernoulli beam with axial force are established and derived to obtain a first-order general estimate of the relative variation of each frequency as a function of the relative variations of the mechanical beam parameters such as axial force, local density and local bending stiffness. The particular case of small localized modifications is addressed. These estimates are used to propose a method to identify the location and quantify a localized variation of the mechanical parameters. A numerical simulation is presented in Section 3 to test the efficiency of the proposed method to localize simultaneous modifications of density and bending stiffness on a beam with axial force variation. In Section 4, the method is applied to experimental data concerning beams without axial force with mass modification or bending stiffness only. Finally, concluding remarks are presented.

2. Presentation of the modifications detection method based on the first-order estimation of frequency relative variations

2.1. Vibration modes of an Euler–Bernoulli beam with axial force

First, several assumptions are made: the beam material is homogeneous, isotropic, and linearly elastic, the axial force (tension) along the beam is constant (positive or null) and damping is ignored. The corresponding partial differential equation governing the transverse deflection $w(x,t)$ of an Euler–Bernoulli beam under axial force is fourth order:

$$\mu(x)\frac{\partial^2 w(x,t)}{\partial t^2}-T\frac{\partial^2 w(x,t)}{\partial x^2}+\frac{\partial^2}{\partial x^2}\left(EI(x)\frac{\partial^2 w(x,t)}{\partial x^2}\right)=p(x,t),\quad x\in[0,L] \tag{1}$$

where $w(x,t)$ is the transverse deflection at point $M(x)$, at time t, $\mu(x)$ the mass per unit length, T the axial force force on the beam, $EI(x)$ the flexural rigidity (or bending stiffness) and $p(x,t)$ the excitation force per unit length. The particular case of the vibrating string where $EI=0$ is not studied here and the case of the Euler–Bernoulli beam without axial force is obtained for $T=0$.

To calculate the normal modes of the problem (Eq. (1)), we have to consider the linear homogeneous equations related to Eq. (1). The normal modes $\phi_n(x)$ are functions which are square integrable on $[0,L]$, as well as $\phi_n'(x)$ and $\phi_n''(x)$ (i.e. $\phi_n(x)\in H^2(0,L)$). By using the method of separation of variables (also known as the Fourier method), it can be shown that the normal modes $\phi_n(x)$ of the beam satisfy the following equation:

$$(EI(x)\phi_n''(x))''-T\phi_n''(x)-\lambda_n\mu(x)\phi_n(x)=0 \tag{2}$$

and some boundary conditions, the most common are listed just below. If the beam is clamped at the abscissa $x=a$ then $\phi_n(a)=\phi_n'(a)=0$. If it is simply supported at $x=a$, then $\phi_n(a)=\phi_n''(a)=0$. For the free end case at $x=L$, we get $\phi_n''(L)=\phi_n^{(3)}(L)=0$ and the axial force is equal to zero.

Multiplying Eq. (2) by any function $u(x)$ belonging to $H^2(0,L)$, an integration by parts leads to the relation:

$$\int_0^L\left(EI(x)\phi_n''(x)u''(x)+T\phi_n'(x)u'(x)-\lambda_n\mu(x)\phi_n(x)u(x)\right)\mathrm{d}x+C=0 \tag{3}$$

with C depending on the boundary conditions:

$$C=\left[\frac{\partial}{\partial x}(EI(x)\phi_n''(x))u(x)\right]_0^L-\left[EI(x)\phi_n''(x)u'(x)\right]_0^L-\left[T\phi_n'(x)u(x)\right]_0^L \tag{4}$$

For a beam satisfying to the boundary conditions indicated above, the quantity C is equal to zero for any function $u(x)$, verifying the same boundary conditions as the modes. Hence, for a beam with standard boundary conditions, the following relation is true:

$$\int_0^L \left(EI(x)\phi_n''(x)u''(x) + T\phi_n'(x)u'(x) - \lambda_n \mu(x)\phi_n(x)u(x) \right) \mathrm{d}x = 0 \tag{5}$$

Using symmetry, it can be proven that the modes are orthogonal with respect to the mass density $\mu(x)$, hence $\forall n \neq k$:

$$\int_0^L \mu(x)\phi_n(x)\phi_k(x)\,\mathrm{d}x = 0 \tag{6}$$

Several ways to norm the modes exist. The modes are often normalized with respect to the mass density, but here, since the mass density may change, no assumptions are made concerning the norm of the modes.

The eigenvalues λ_n depend on the ratio $EI(x)/T$. More precisely, choosing $u(x) = \phi_n(x)$ in Eq. (5), we conclude

$$\int_0^L EI(x)\phi_n''^2(x)\,\mathrm{d}x + T\int_0^L \phi_n'^2(x)\,\mathrm{d}x - \lambda_n \int_0^L \mu(x)\phi_n^2(x)\,\mathrm{d}x = 0 \tag{7}$$

For an axial force not null, a parameter $\gamma_n > 0$ is introduced such that

$$\gamma_n = \frac{\int_0^L EI(x)\phi_n''^2(x)\,\mathrm{d}x}{T\int_0^L \phi_n'^2(x)\,\mathrm{d}x} \tag{8}$$

For a string, EI is null and so $\gamma_n = 0$. Using Eq. (7), the eigenvalue λ_n can be written as a function of γ_n and either of the axial force or the bending stiffness:

$$\lambda_n = T(1+\gamma_n)\frac{\int_0^L \phi_n'^2(x)\,\mathrm{d}x}{\int_0^L \mu(x)\phi_n^2(x)\,\mathrm{d}x} = \frac{1+\gamma_n}{\gamma_n}\frac{\int_0^L EI(x)\phi_n''^2(x)\,\mathrm{d}x}{\int_0^L \mu(x)\phi_n^2(x)\,\mathrm{d}x} \tag{9}$$

Choosing $u(x) = \phi_k(x)$, $\forall k \neq n$ in Eq. (5) and using the relation (6), we get

$$\int_0^L EI(x)\phi_n''(x)\phi_k''(x)\,\mathrm{d}x + T\int_0^L \phi_n'(x)\phi_k'(x)\,\mathrm{d}x = 0 \tag{10}$$

When T tends towards 0, γ_n tends towards infinity and relations (9) and (10) for a beam without axial force result in these equations:

$$T = 0, \quad \lambda_n = \frac{\int_0^L EI(x)\phi_n''^2(x)\,\mathrm{d}x}{\int_0^L \mu(x)\phi_n^2(x)\,\mathrm{d}x}, \quad \int_0^L EI(x)\phi_n''(x)\phi_k''(x)\,\mathrm{d}x = 0 \tag{11}$$

This shows the orthogonality of the curvature mode shapes with respect to the flexural rigidity for a beam without axial force.

2.2. Modal parameter variations due to mechanical characteristic modifications

2.2.1. General case

In the following section, we consider changes in intrinsic characteristics of the beam due to local reduction or increase in flexural rigidity and mass density combined with global axial force variation. The modifications made in this study to the flexural rigidity and/or to the mass density will be internal and the modifications to the axial force will be external. These modifications are assumed to be small enough to calculate a first-order estimate. Hereafter, we study the variation in the modal parameters due to these modifications.

The modified mass and flexural rigidity are denoted by $\tilde{EI}(x)$ and $\tilde{\mu}(x)$ with

$$\tilde{EI}(x) = EI(x) + \Delta EI(x) \tag{12}$$

$$\tilde{\mu}(x) = \mu(x) + \Delta\mu(x) \tag{13}$$

where the variation of the density and the bending stiffness are denoted by $\Delta\mu(x)$ and $\Delta EI(x)$ respectively. The axial force is assumed to be constant along the beam. The change in axial force is denoted by ΔT and the modified axial force is equal to

$$\tilde{T} = T + \Delta T \tag{14}$$

These changes result in new mode shapes and new eigenvalues:

$$\tilde{\phi}_n(x) = \phi_n(x) + \Delta\phi_n(x) \tag{15}$$

$$\tilde{\lambda}_n = \lambda_n + \Delta\lambda_n \tag{16}$$

For any function $u(x) \in H^2(0, L)$ within the boundary conditions, the new normal modes $\tilde{\phi}_n(x)$ must satisfy relation (5):

$$\int_0^L \left(\tilde{EI}(x)\tilde{\phi}_n''(x)u''(x) + \tilde{T}\tilde{\phi}_n'(x)u'(x) - \tilde{\lambda}_n\tilde{\mu}(x)\tilde{\phi}_n(x)u(x) \right) \mathrm{d}x = 0 \tag{17}$$

As we want to compute a first-order estimation, the following approximation is made for each n:

$$\tilde{\lambda}_n\tilde{\mu}(x)\tilde{\phi}_n(x) - \lambda_n\mu(x)\phi_n(x) \approx \lambda_n\mu(x)\Delta\phi_n(x) + (\Delta\lambda_n\mu(x) + \lambda_n\Delta\mu(x))\phi_n(x) \tag{18}$$

The same type of approximation is made for T, $\tilde{T}\tilde{\phi}_n(x) - T\phi_n(x) = \tilde{T}\Delta\phi_n(x) + \Delta T\phi_n(x) \approx T\Delta\phi_n(x) + \Delta T\phi_n(x)$, as well as for $EI(x)$.

Moreover the change in mode shapes, $\Delta\phi_n(x)$, can be expressed using the normal modes basis $\{\phi_k\}_{k=1}^{\infty}$, as

$$\Delta\phi_n(x) = \sum_{k=1}^{\infty} \alpha_{nk}\phi_k(x) \tag{19}$$

By subtracting Eq. (5) to Eq. (17), and after some calculations given in Appendix A, the λ_n relative variation can be expressed as

$$\frac{\Delta\lambda_n}{\lambda_n} \approx \frac{\gamma_n}{1+\gamma_n}\frac{\int_0^L \Delta EI(x)\phi_n''^2(x)\,\mathrm{d}x}{\int_0^L EI(x)\phi_n''^2(x)\,\mathrm{d}x} + \frac{\Delta T}{T}\frac{1}{(1+\gamma_n)} - \frac{\int_0^L \Delta\mu(x)\phi_n^2(x)\,\mathrm{d}x}{\int_0^L \mu(x)\phi_n^2(x)\,\mathrm{d}x} \tag{20}$$

For a beam without axial force, it gives

$$T = 0, \quad \frac{\Delta\lambda_n}{\lambda_n} \approx \frac{\int_0^L \Delta EI(x)\phi_n''^2(x)\,\mathrm{d}x}{\int_0^L EI(x)\phi_n''^2(x)\,\mathrm{d}x} - \frac{\int_0^L \Delta\mu(x)\phi_n^2(x)\,\mathrm{d}x}{\int_0^L \mu(x)\phi_n^2(x)\,\mathrm{d}x} \tag{21}$$

2.2.2. Case of localized modifications

The external modifications (of mass and/or bending stiffness) are assumed to be localized around x_0 on the interval Ω of length ΔL with ΔL very small with respect to L, the total length of the beam. The integrals $\int_0^L \Delta EI(x)\phi_n''^2(x)\,\mathrm{d}x$ and $\int_0^L \Delta\mu(x)\phi_n^2(x)\,\mathrm{d}x$ can be replaced by $\left(\int_\Omega \Delta EI(x)\,\mathrm{d}x\right)\phi_n''^2(x_0)$ and $\left(\int_\Omega \Delta\mu(x)\,\mathrm{d}x\right)\phi_n^2(x_0)$, respectively. Moreover, because λ_n varies with the square of the frequency f_n, $2\frac{\Delta f_n}{f_n} = \frac{\Delta\lambda_n}{\lambda_n}$. The relative variation of each natural frequency, considered as a function of x_0, can be deduced from Eq. (20):

$$2\frac{\Delta f_n}{f_n}(x_0) \approx \frac{\gamma_n}{1+\gamma_n}\frac{\left(\int_\Omega \Delta EI(x)\,\mathrm{d}x\right)\phi_n''^2(x_0)}{\int_0^L EI(x)\phi_n''^2(x)\,\mathrm{d}x} + \frac{\Delta T}{T}\frac{1}{(1+\gamma_n)} - \frac{\left(\int_\Omega \Delta\mu(x)\,\mathrm{d}x\right)\phi_n^2(x_0)}{\int_0^L \mu(x)\phi_n^2(x)\,\mathrm{d}x} \tag{22}$$

The modifications can be discontinuous or continuous. So the functions $\Delta EI(x)$ and $\Delta\mu(x)$ may have different forms. If the bending stiffness and the density are assumed to be initially constant ($EI(x) = EI$ and $\mu(x) = \mu$), and simple rectangular functions are used ($\Delta EI(x) = \Delta EI$, $\Delta\mu(x) = \Delta\mu$ on Ω), Eq. (22) can be

rewritten as

$$2\frac{\Delta f_n}{f_n}(x_0) \approx \frac{\gamma_n}{1+\gamma_n}\frac{\Delta EI\Delta L}{EI}\frac{\phi_n''^2(x_0)}{\|\phi_n''\|_2^2} + \frac{\Delta T}{T}\frac{1}{(1+\gamma_n)} - \frac{\Delta\mu\Delta L}{\mu}\frac{\phi_n^2(x_0)}{\|\phi_n\|_2^2} \quad (23)$$

This relation is established for each mode. It creates a link between the frequency variation ratio and the variation ratios of bending stiffness, mass density and axial force, assuming the corresponding initial mode shape and first two mode shape derivatives are known. This relation can be rewritten as

$$\frac{\Delta f_n}{f_n}(x_0) \approx \frac{1}{2(1+\gamma_n)}\frac{\Delta T}{T} + G_n(x_0)\frac{\Delta EI\Delta L}{EIL} - H_n(x_0)\frac{\Delta\mu\Delta L}{\mu L}$$

$$\text{with} \quad G_n(x) = \frac{\gamma_n}{2(1+\gamma_n)}\frac{L\phi_n''^2(x)}{\|\phi_n''\|_2^2} \quad \text{and} \quad H_n(x) = \frac{1}{2}\frac{L\phi_n^2(x)}{\|\phi_n\|_2^2} \quad (24)$$

For usual boundary conditions and an initially uniform beam, the analytical form of the mode shapes is known [28]. Thus, for a simply supported beam at its ends, with or without axial force, the expression of normal modes is simple: $\phi_n(x) = \sigma_n \sin\left(\frac{n\pi x}{L}\right)$. It can be noticed that they are similar to the normal modes of the vibrating string clamped at both ends and independent of the axial force T.

The expression of the parameter γ_n given in Eq. (8) can then be calculated as

$$\gamma_n = (n\pi)^2\frac{EI}{T\,L^2} = (n\pi)^2\xi^2 \quad \text{with } \xi^2 = \frac{EI}{T\,L^2} \quad (25)$$

and the expression of Eq. (24) becomes

$$\frac{\Delta f_n}{f_n}(x_0) \approx \frac{1}{2(1+\gamma_n)}\frac{\Delta T}{T} + \left(\frac{\Delta EI\Delta L}{EIL}\frac{\gamma_n}{(1+\gamma_n)} - \frac{\Delta\mu\Delta L}{\mu L}\right)\sin^2\left(\frac{n\pi x_0}{L}\right) \quad (26)$$

where the first term containing the relative variation of the axial force is usually linked to external variation (for cables on a bridge: traffic, wind, etc.) and the second one concerns local and physical modifications.

It is noteworthy that, away from the ends, the mode shapes for clamped or simply supported boundary conditions are quite similar to the mode shapes of a simply supported beam at its ends, and so if the modification of density and bending stiffness are assumed to be sufficiently far from the ends, the estimation (26) established for a simply supported beam at its ends remains a correct approximation. More details concerning the previous simplifications are given in [28].

2.3. Localization and estimation of the modifications

The aim of this section is to localize modifications using the relation (24) for the variation of each frequency. We assume that the first p frequencies of two states of the beam, the initial state and the modified one are known, and that, for the initial state, the corresponding mode shapes and first two mode shape derivatives are identified. The modifications of the mass and bending stiffness are assumed to be localized around the abscissa x_0 on a small interval of length ΔL (with $\Delta L \ll L$). For the sake of simplicity, the modifications are assumed constant on the interval $[x_0 - \frac{\Delta L}{2}, x_0 + \frac{\Delta L}{2}]$.

In the relation (24), the terms $\frac{\Delta T}{T}$, $\frac{\Delta EI\Delta L}{EIL}$ and $\frac{\Delta\mu\Delta L}{\mu L}$ are unknown and represent the relative variation of axial force, bending stiffness and mass, respectively.

To localize the modification, Eq. (24) is written for four different frequencies k, m, n, q. These four equations with three unknowns must be compatible, hence the corresponding fourth order determinant formed by the coefficients should be equal to zero. So, with $\beta_n = \frac{1}{2(1+\gamma_n)}$, the function $F_{k,m,n,q}(x)$ is defined by

$$F_{k,m,n,q}(x) = \begin{vmatrix} \frac{\Delta f_k}{f_k}(x) & -\beta_k & -G_k(x) & H_k(x) \\ \frac{\Delta f_m}{f_m}(x) & -\beta_m & -G_m(x) & H_m(x) \\ \frac{\Delta f_n}{f_n}(x) & -\beta_n & -G_n(x) & H_n(x) \\ \frac{\Delta f_q}{f_q}(x) & -\beta_q & -G_q(x) & H_q(x) \end{vmatrix} \quad (27)$$

This function $F_{k,m,n,q}(x)$ should be null for $x = x_0$. The value x_0 is a minimizer of $|F_{k,m,n,q}(x)|$ for any (k, m, n, q). If the first four eigenfrequencies are measured before and after the modifications, and if the corresponding initial mode shapes and their first two derivatives are known, then it is possible to evaluate x_0 as $x_m = \arg\min_x F_{1,2,3,4}(x)$. If eigenvalues of higher order are also known, it is possible to improve the identification of x_0 by taking into account this additional information. Thus if the first p eigenfrequencies (with $p \geq 4$) are available, the possible values of x_0 can be obtained as the values of x that minimize the quantity $Q_p(x)$ defined below:

$$Q_p(x) = \sum_{1 \leq k < m < n < q \leq p} |F_{k,m,n,q}(x)| \quad (28)$$

It should be noted that for a fixed value of x, the quantity $Q_p(x)$ increases as the number p of used frequencies increases. We will show that, in case of a single modification, the maximum of the function $Q_p(x)$ is linked to the amplitude of the modification whereas the normalized function $\widehat{Q}_p(x) = Q_p(x)/\|Q_p\|_\infty$ only depends on the type of the modification. Theoretically $\widehat{Q}_p(x_0) = 0$, hence an estimation x_m of the localization is calculated with

$$x_m = \arg\min_x \widehat{Q}_p(x). \quad (29)$$

It will be observed that, in general, the accuracy of the localization of x_0 increases with the number p of eigenmodes taken into account.

Once x_0 is estimated by x_m, the coefficients $G_n(x_0)$ and $H_n(x_0)$ can be replaced by $G_n(x_m)$ and $H_n(x_m)$ in (24) for $n = 1, \ldots, p$. Then the unknown relative variations of axial force ($\frac{\Delta T}{T}$), bending stiffness ($\frac{\Delta EI\Delta L}{EIL}$), and mass ($\frac{\Delta\mu\Delta L}{\mu L}$) can be calculated by a linear least squares approximation.

The boundary conditions and the location of the modification with respect to the ends of the beam have an influence on the localization of x_0. The sensitivity of the localization with respect to these factors will be studied in Section 4.

In the next section, the proposed method of localization based on the use of $Q_p(x)$ is applied to numerical data in case of a beam with three simultaneous modifications. Then the relative variations of the mechanical parameters are estimated.

3. Numerical application to a beam with axial force

To check the efficiency of the proposed method on a generic beam undergoing simultaneous variations in axial force, bending stiffness, and mass, the case of a clamped–clamped beam simulated by finite element method is addressed. As a pre-stressed aluminum beam has been already used for quasi-stationary and non-stationary tests [29], the same characteristics are chosen for this finite element simulation: length $L = 0.440$ m, section $S = b \times h = 0.025$ m $\times$ 0.002 m, Young modulus $E = 69$ GPa, density $\rho = 2700$ kg m^{-3}, and total mass $m = 0.0594$ kg. (This pre-stressed beam was chosen because the structural behavior is similar to cables and the experiments were easier to perform.)

The beam is then meshed into 500 finite beam elements of 8.8 $\times 10^{-4}$ m length each. The modification is localized between $x_a = 0.1170$ m and $x_b = 0.1232$ m, corresponding to a central

position of $x_0=0.1201$ m. The part with the modifications is 0.0062 m long and meshed with 7 beam elements, so $\frac{\Delta L}{L}=0.014$. On this interval, the bending stiffness and the density are modified: $\frac{\Delta EI}{EI}=-5\%$ and $\frac{\Delta\mu}{\mu}=-5\%$ corresponding to a loss of the total mass of around 0.06%. The axial force, tension in our case, is also modified: the initial tension is $T=2000$ N and the modified one is chosen to be equal to $\tilde{T}=1980$ N so $\frac{\Delta T}{T}=-1\%$. This corresponds to a simultaneous loss of mass, bending stiffness, and axial force. The first six frequencies are numerically determined and listed in Table 1.

3.1. Localization of the modification

In this case, there are three unknown modifications. To localize the modifications of mass and bending stiffness, we should use the function $Q_p(x)$ defined in Eq. (28), which depends on p frequencies (with $p\geq 4$) and on the corresponding mode shapes and first two mode shape derivatives of the initial state. The functions $Q_p(x)$ are plotted for the first half of the beam in Fig. 1(a) for $p=4$, 5, and 6. It appears that for these three unknown modifications, the localization is quite accurate when six modes are considered.

The symmetry of the function Q_p, and so the presence of two minima, is due to the symmetry of the initial problem (clamped–clamped beam). One of these minima is located at the abscissa $x_m=0.1198$ m which is very close to the position of the modification $x_0=0.1201$ m. This limitation comes from the fact that all the terms depending on the mode shapes or the first two mode shape derivatives are square. So, if the boundary conditions are identical at both ends of the beam, two minima are obtained. However, this problem of two possible localizations for one modification has already been addressed in [30], with the use of antiresonances. The use of mode shapes of the modified beam could also help us to determine the correct localization. Practically, the two possible zones can be checked locally using complementary measures.

3.2. Quantification of mass, bending stiffness, and axial force variations

As previously said, replacing the coefficients $G_n(x_0)$ and $H_n(x_0)$ for a clamped–clamped beam with mechanical parameters EI, μ, and T, by $G_n(x_m)$ and $H_n(x_m)$ in (24) for $n=1$–6 (Table 2), and using a least squares procedure leads to an estimation of $\frac{\Delta EI\Delta L}{EIL}$, $\frac{\Delta\mu\Delta L}{\mu L}$, and $\frac{\Delta T}{T}$ and then to $\frac{\Delta EI}{EI}$ and $\frac{\Delta\mu}{\mu}$, as $\Delta L/L$ is known in this numerical case.

The modifications estimated by least squares procedure are $\frac{\Delta EI}{EI}=-5.14\%$, $\frac{\Delta\mu}{\mu}=-4.96\%$, and $\frac{\Delta T}{T}=-1.004\%$, which are very close to the imposed modifications.

In Section 4, this method is then applied to experimental data concerning only one structural modification and without axial forces.

4. Application to experimental data without axial force and only one structural modification

Two cases are presented: one concerns the localization and estimation of a localized additional mass, the other the localization and quantification of the variation of the bending stiffness due to a notch.

In the first case, experiments have been performed on an aluminum clamped–clamped beam, with or without the addition of a localized mass. The beam responses after shock have been measured and processed through Cauchy wavelet transform [31] in order to obtain modal parameters of both the unmodified and the modified beam. It is worthwhile to remember that the mode shapes of the modified structure are not useful for our technique.

In the second case, our method has been applied to experimental data found in the literature and the results have been compared with those of other techniques [28,32]. Two different experiments are considered here: the first concerns a beam with free–free boundary conditions [21] and the second concerns a cantilever beam [25]. In both cases, only the natural frequencies of

Table 1
Numerical frequencies (in Hz) before and after modifications and frequency relative variation for a clamped–clamped beam under tension.

f_n	Healthy	Modified	$\Delta f_n/f_n$ (%)
f_1	157.49	156.88	−0.39
f_2	328.01	326.95	−0.32
f_3	522.37	520.73	−0.31
f_4	748.44	746.24	−0.29
f_5	1011.44	1009.15	−0.23
f_6	1314.80	1312.43	−0.18

Table 2
Values of $\beta_n=1/(2+2\gamma_n)$, $G_n(x_m)$, and $H_n(x_m)$ for the first sixth frequencies of a clamped–clamped beam under tension and $x_m=0.1198$ m.

n	β_n	$G_n(x_m)$	$H_n(x_m)$
1	0.424	0.017	0.541
2	0.388	0.133	1.089
3	0.340	0.125	0.531
4	0.292	0.001	0.001
5	0.247	0.274	0.595
6	0.209	0.548	1.004

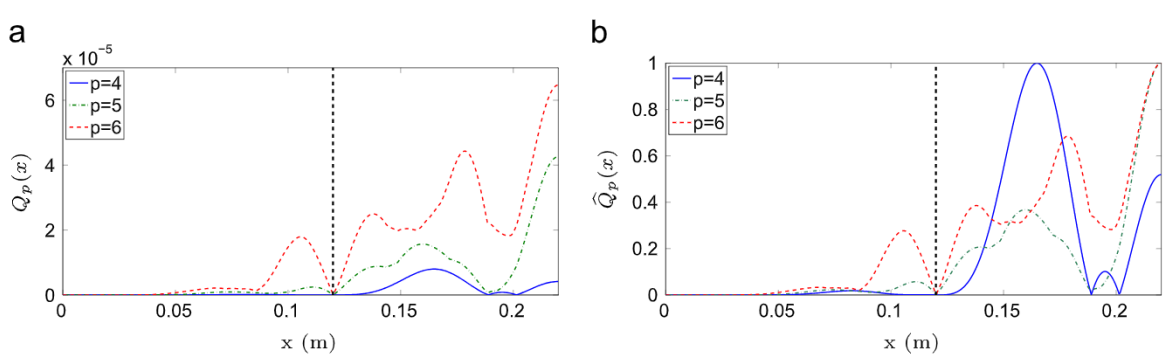

Fig. 1. Graphs of (a) $Q_p(x)$ and (b) $\widehat{Q}_p(x)$, with $p=4$–6, for a beam under tension and modifications around $x_0=0.120$ m. Vertical dotted line indicates the location of the modifications. Due to the symmetry of the initial problem and because the square of the initial mode shapes and first two mode shape derivatives are even functions with respect to the mid-point of the beam, the functions are plotted for the first half of the beam. With three unknowns, at least five frequencies are necessary to localize the position of the modifications.

the modified structure are taken from the literature; the mode shapes of the unmodified structure are numerically calculated from Eq. (2) with the boundary conditions and geometrical and mechanical characteristics of beams that are given in literature. The free–free beam will be used to compare the efficiency of our localization and quantification method to the method proposed by Morassi [21]. The cantilever beam studied by Agarwalla [25] will be used to investigate the influence of the modification position on the efficiency of the method and to propose an improvement in the case of a modification close to the free end and hence, more difficult to localize.

4.1. Mass variation localization and quantification on a clamped–clamped beam

The dimensions of the beam are length $L=0.705$ m, section $S=b\times h=0.04\ \text{m}\times 0.008$ m, Young modulus $E=69$ GPa, density $\rho=2700\ \text{kg m}^{-3}$, and total mass $m=0.637$ kg. A hole was drilled in the beam at the abscissa $x_0=0.321$ m, at half width. Then, a threaded shaft is clamped on the beam, through the hole, with two washers and two hex nuts (Nominal size M5). In order to add mass, without changing the stiffness of the beam, other hex nuts are added on the threaded shaft (Fig. 2). The beam with the threaded shaft, two washers and two hex nuts is considered as the initial state of the beam. The first modification state corresponds to the addition from the healthy state of two hex nuts on the threaded shaft, one on each side of the beam, corresponding to a mass variation $\Delta m_1/m=\Delta\mu_1\Delta L/\mu L$ of 0.31%. Two other hex nuts are added to this first case for the second modification case leading to $\Delta m_2/m=0.62\%$. The different states are illustrated in Fig. 2.

To identify the modal parameters necessary to the method (e.g. eigenfrequencies and mode shapes), the beam was instrumented with 11 accelerometers. For each case (without mass modification or initial, states 1 and 2), 10 dynamic impact tests were performed. The free decay responses of the accelerometers were processed by a modal identification method based on the use of continuous wavelet transform [31]. This technique has been used to check the linearity of the beam behavior. The time evolution of the first instantaneous frequencies remains constant for the duration of test carried out, showing that the behavior of the beam remains linear during the experiments [33]. For the healthy state, the experimental mode shapes obtained are used to scale theoretical mode shapes with a least squares optimization process. Then, theoretical mode shapes and first two derivatives mode shapes are used for the localization procedure. Table 3 presents the first six frequencies calculated by average of the frequencies obtained for all accelerometers, except those close to mode shape nodes and to the embedments, and for the ten dynamic tests. The frequency relative variations between the mass modification states and the initial state are also indicated as well as the standard deviations of the frequencies, σ_i, obtained in the same way as the frequencies.

In these experiments, the only unknown quantity is the relative variation of the mass, so the relation (24) becomes

$$\frac{\Delta f_n}{f_n}(x_0)\approx -H_n(x_0)\frac{\Delta\mu\Delta L}{\mu L}\quad \text{with } H_n(x_0)=\frac{L\phi_n^2(x_0)}{2\|\phi_n\|_2^2} \tag{30}$$

The function $F_{m,n}$ is then defined by

$$F_{m,n}(x)=\frac{\Delta f_n}{f_n}H_m(x)-\frac{\Delta f_m}{f_m}H_n(x) \tag{31}$$

In our method, to take into account the measurements obtained for other low frequencies the function $Q_p(x)$ is introduced, which permits to obtain more precise results concerning the localization:

$$Q_p(x)=\sum_{1\le n<m\le p}|F_{m,n}(x)| \tag{32}$$

As in the general case, an estimate of the localization can be obtained by $x_m=\arg\min_x\widehat{Q}_p(x)$ where $\widehat{Q}_p(x)=\frac{Q_p(x)}{\|Q_p\|_\infty}$ is the normalized function of $Q_p(x)$. An indication of the magnitude of the modification will be given by the maximum of the function $Q_p(x)$.

In the case of one mass modification, the use of two eigenfrequencies is sufficient to eliminate the single unknown.

For both cases of mass modification, the normalized functions based on Eq. (28) for $p=2$–6 are depicted in Fig. 3 ($\Delta m_1/m$ on the left and $\Delta m_2/m$ on the right). We should recall that, due to the symmetry of boundary conditions, the functions are plotted for the first half of the beam.

The locations of the mass variation obtained by the localization procedure for the two cases are $x_{m_1}=0.324$ m and $x_{m_2}=0.319$ m, which is very close to the real position ($x_0=0.321$ m) especially as the hex nuts width is a few millimeters. However, the localization of the modification is less obvious for the first variation of mass as a clear minimum is observed in the normalized function curves only for $p=4$ and 6. This can be explained by the fact that the change in mass is very low and close to the center of the beam, therefore close to a node of even mode shapes.

Then, from these locations, the mass variations are estimated using a least mean squares approximation (Table 4). The results are very close to the real mass variation which validates the proposed method experimentally for mass changes.

Table 3
Experimental frequencies (in Hz), frequency relative variations $\Delta f_n/f_n$ (in parentheses, in %) and standard deviations (in Hz) for a clamped–clamped beam with two variations of mass at $x_0=0.321$ m.

f_n	Healthy	σ_0 (Hz)	$\Delta m_1/m=0.31\%$	σ_1 (Hz)	$\Delta m_2/m=0.62\%$	σ_2 (Hz)
f_1	74.68	0.010	74.50 (−0.24)	0.005	74.22 (−0.62)	0.002
f_2	207.40	0.027	207.40 (0.00)	0.005	207.26 (−0.07)	0.005
f_3	402.39	0.005	401.65 (−0.18)	0.008	400.81 (−0.39)	0.007
f_4	678.70	0.085	677.97 (−0.11)	0.115	676.79 (−0.28)	0.080
f_5	1006.63	0.081	1004.68 (−0.19)	0.049	1003.27 (−0.33)	0.061
f_6	1394.38	0.157	1391.89 (−0.18)	0.153	1389.03 (−0.38)	0.184

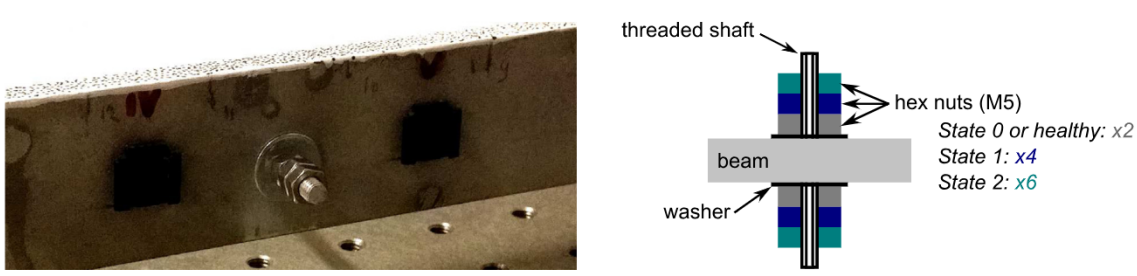

Fig. 2. Experimental tests for mass variation quantification on a clamped–clamped beam. The initial state of the beam includes, with the threaded shaft, two washers and two hex nuts. For the first modification case, two hex nuts are added to the initial state ($\Delta m_1/m=0.31\%$) and two others for the second state ($\Delta m_2/m=0.62\%$).

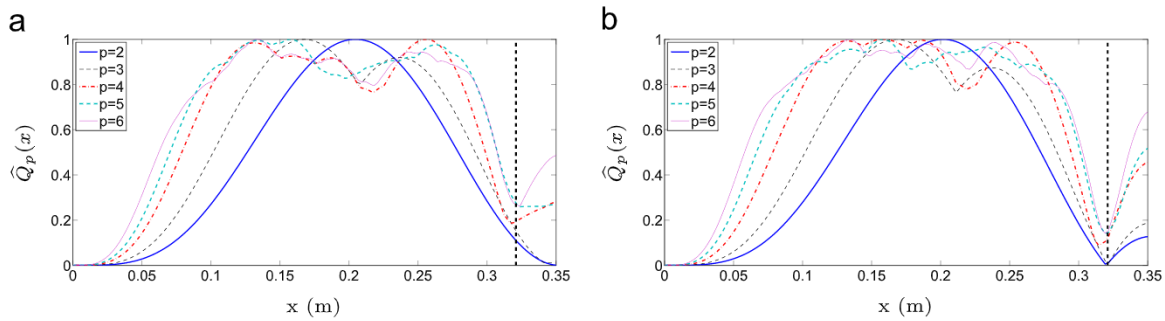

Fig. 3. Normalized function $\widehat{Q}_p(x)$ ($p=2$ to 6) for the two mass modifications: (a) Δm_1 and (b) Δm_2. Vertical dotted line indicates the location of the nuts. The minimum of the functions becomes sharper when the number of frequencies used increases. For the larger addition of mass ($\Delta m_2/m=0.62\%$), two frequencies are enough to localize the nuts. For a smaller addition of mass ($\Delta m_1/m=0.31\%$), more frequencies are needed (at least four).

Table 4
Quantification of the mass variation for the two modification cases.

Mass variation	Real (%)	Estimated (%)
$\Delta m_1/m$	0.31	0.30
$\Delta m_2/m$	0.62	0.66

4.2. Stiffness change localization and quantification on free–free and cantilever beams

In this section, the only unknown quantity is the relative variation of the bending stiffness. The relation (24) yields in this case

$$\frac{\Delta f_n}{f_n}(x_0) \approx G_n(x_0)\frac{\Delta EI\Delta L}{EIL} \quad \text{with } G_n(x_0)=\frac{L\phi_n''^2(x_0)}{2\|\phi_n''\|_2^2} \tag{33}$$

In the case of a single unknown, the function $F_{m,n}$ is the determinant of the system obtained for the two frequencies m and n:

$$F_{m,n}(x)=\frac{\Delta f_n}{f_n}G_m(x)-\frac{\Delta f_m}{f_m}G_n(x) \tag{34}$$

As previously, the use of the two first eigenfrequencies is sufficient to eliminate the single unknown and to obtain a relation between the variation of two frequencies and the localization x_0, thus we get in this case:

$$\frac{\Delta f_2}{\Delta f_1}(x_0) \approx \frac{\phi_2''^2(x_0)}{\phi_1''^2(x_0)} \tag{35}$$

This relation (35) has been used by Morassi in [34] concerning a rod. Then the same type of idea was used for beam or even for pipeline. Our procedure permits to take advantage of the knowledge of the variation of more frequencies.

4.2.1. Localization and quantification of a notch for a free–free beam – Comparison of results with another technique

Now we want to compare our method and the method used by Morassi [21] for a free–free beam. The beam was suspended from above by two soft springs, to simulate free–free boundary conditions. The damage consisted of two symmetric notches of width 1.5 mm, located at the cross-section 0.225 m from the left end (see Fig. 4). Their depth was progressively increased by 1 mm at a time from the undamaged configuration to a final level of damage corresponding to a depth of 6 mm on both sides of the cross-section. It should be recalled that the free–free beam has a double multiplicity zero eigenvalue, corresponding to two independent rigid body motions. The rigid body modes are insensitive to damage and will be omitted. For each level, the lowest seven natural frequencies were measured using an impulse technique [21] (Table 5).

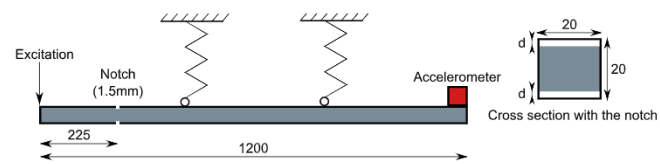

Fig. 4. Experimental model of bending vibrating beam and damage configuration (lengths in mm).

The aim of Morassi [21] was to localize the modification by estimating the bending stiffness along the beam using Fourier type series. The partial development uses between two and seven frequencies. The notch is supposed to correspond to the minimal value of the bending stiffness. The results for a notch of 3 mm depth are shown in Fig. 5. The localization is approximatively obtained for $p=3$, 4, and 5 but completely fails for $p=2$, 6, and 7. Disturbances begin to appear in the estimation of the bending stiffness as the number of frequencies used increases. Moreover, this method does not succeed in localizing small defects of 1 or 2 mm.

We now apply our method to this case of a free–free beam with a 3 mm notch. The graphs of $Q_p(x)$ and of the normalized function $\widehat{Q}_p(x)$ are depicted for $p=3$, 4, 5, 6, and 7 in Fig. 6. Due to the symmetry of the initial problem, the square of the initial mode shapes and curvature mode shapes are even functions with respect to the mid-point of the beam and thus two symmetric minima can be observed.

The value of the estimated position of the modification x_m depends on the number of used frequencies p. These values are presented in Table 6. The accuracy of the localization of x_m is rather good since the error is less than 10 mm for a beam of 1200 mm long.

For a depth d varying from 1 mm to 6 mm, the values of the localizations x_m^d, obtained for the different depths and for $p=7$, are given in Table 7. The localization is rather accurate: the error is less than 3 mm for depths less than 5 mm and a little bit more for the largest depth $d=6$ mm (two notches of 6 mm are quite large with respect to the total cross section of 20 mm).

The question is now to evaluate the size of the modification. Once x_0 has been estimated by x_m^d, the coefficients $G_n(x_0)$ can be replaced by $G_n(x_m^d)$ in (33) for $n=1,\ldots,p$ (Table 8).

The relative variations of the bending stiffness $\frac{\Delta EI\Delta L}{EIL}$ can be obtained as the quotient of $\frac{\Delta f_n}{f_n}$ by $G_n(x_m^d)$. As seven equations (Eq. (33)) are available, one for each mode, we tested different combinations of modes among these equations to perform a linear least squares approximation. The results are presented in Table 9 and are rather similar regardless of the combination, showing the robustness of the approximation. However, in order to avoid high relative errors, we prefer to consider only those equations for which the denominator $G_n(x_m^d)$ is not too small. The chosen

Table 5
Experimental frequencies (in Hz) and frequency relative variations $\Delta f_n/f_n$ (in parentheses, in %) for a free–free beam when the depth d of the notch is varying. Taken from Morassi [21].

f_n	Healthy	$d=1$ mm	$d=2$ mm	$d=3$ mm	$d=4$ mm	$d=5$ mm	$d=6$ mm
f_1	72.19	72.19 (0.00)	72.16 (−0.04)	72.16 (−0.04)	72.06 (−0.18)	71.94 (−0.35)	71.53 (−0.91)
f_2	198.4	198.3 (−0.05)	198.1 (−0.17)	197.7 (−0.36)	196.4 (−0.99)	194.7 (−1.87)	189.3 (−4.61)
f_3	387.7	387.5 (−0.06)	386.8 (−0.23)	385.3 (−0.62)	381.6 (−1.59)	374.9 (−3.29)	361.0 (−6.90)
f_4	639.7	639.4 (−0.05)	638.4 (−0.20)	636.3 (−0.54)	630.8 (−1.39)	623.8 (−2.49)	607.0 (−5.11)
f_5	951.5	951.3 (−0.02)	950.8 (−0.08)	950.0 (−0.15)	947.0 (−0.47)	943.5 (−0.84)	935.2 (−1.71)
f_6	1320.6	1320.6 (0.00)	1320.3 (−0.02)	1320.3 (−0.02)	1320.0 (−0.04)	1320.0 (−0.04)	1319.2 (−0.11)
f_7	1747.0	1746.8 (−0.01)	1746.6 (−0.02)	1746.1 (−0.05)	1742.9 (−0.24)	1739.4 (−0.44)	1728.3 (−1.07)

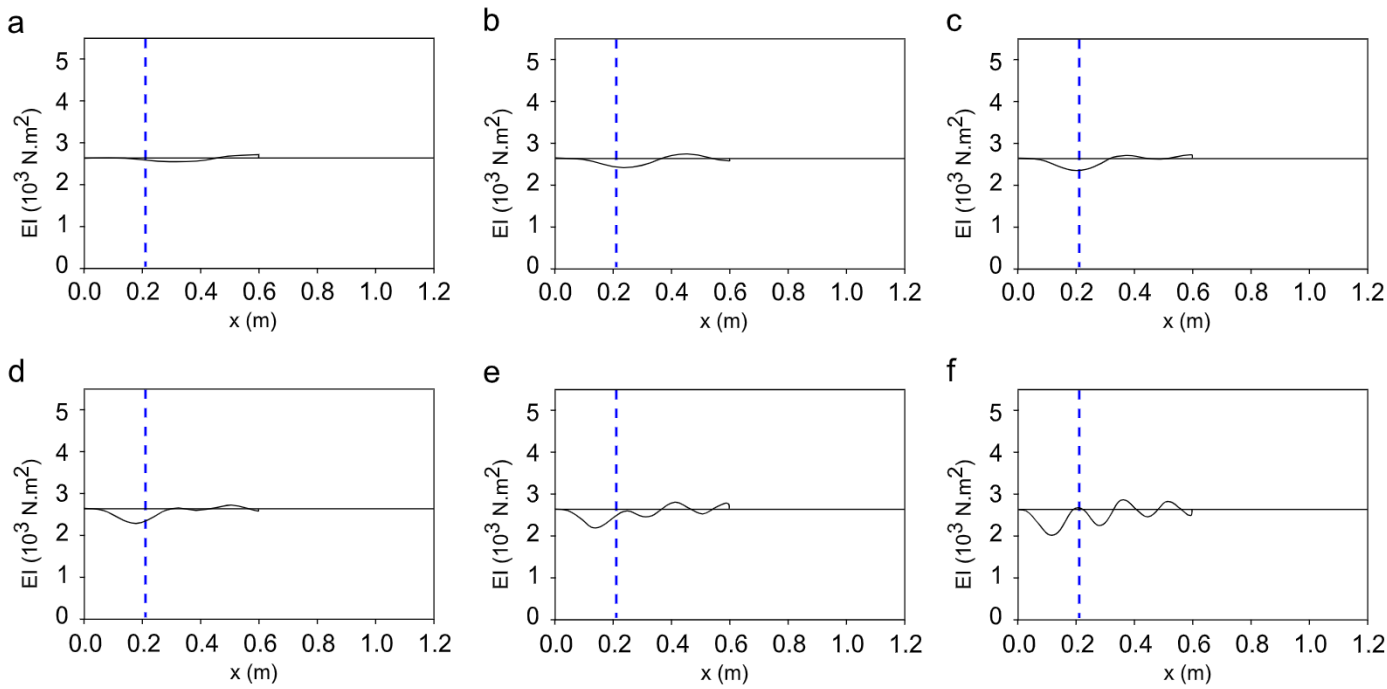

Fig. 5. Estimated bending stiffness (EI) for 3 mm notch with damage location at $x_0=0.225$ m and p frequencies used: (a) $p=2$, (b) $p=3$, (c) $p=4$, (d) $p=5$, (e) $p=6$, and (f) $p=7$, taken from Morassi [21]. Vertical dotted line indicates the location of the notch. The results obtained by the method proposed in [21] are quite accurate only with four frequencies used (c).

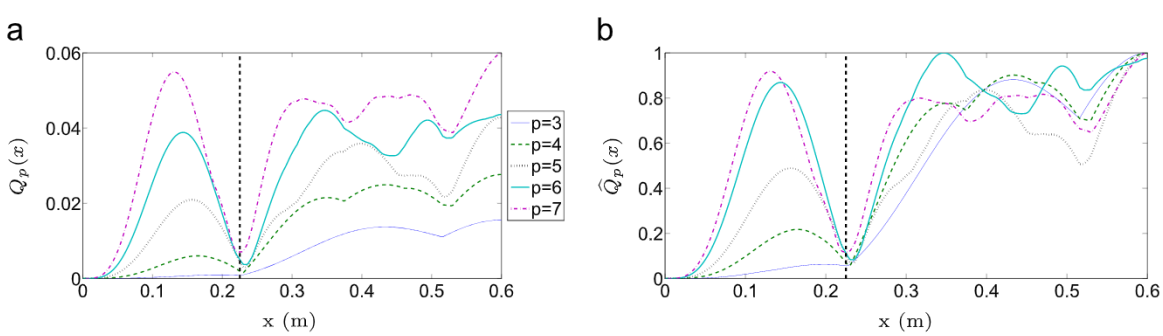

Fig. 6. Graphs of (a) $Q_p(x)$ and (b) $\widehat{Q}_p(x)$ for a notch of 3 mm depth at $x_0=0.225$ m with p frequencies used, from 3 to 7. Vertical dotted line indicates the location of the notch. The localization of the modification is accurate from three frequencies and the minimum of the functions becomes sharper when the number of frequencies used increases.

Table 6
Localization of x_m for a notch of 3 mm depth at $x_0=0.225$ m and p frequencies used ($p=3$–7).

p	3	4	5	6	7
x_m (m)	0.226	0.230	0.233	0.235	0.223

Table 7
Localization of x_m for a notch of depth d (1–6 mm) at $x_0=0.225$ m and $p=7$ frequencies used.

d (mm)	1	2	3	4	5	6
x_m (m)	0.228	0.228	0.223	0.226	0.226	0.233

combination is that comprising all modes except the sixth (in bold in Table 9). Fig. 7 illustrates the relative variations of the bending stiffness, $\frac{\Delta EI \Delta L}{EIL}$, depending on the notch depth d for this case. A cubic trend of the relative variations of the bending stiffness to the notch depth is observed as expected. Indeed, for a beam with a rectangular cross section, $\Delta EI = \frac{b \cdot (h-d)^3}{12} - \frac{b \cdot h^3}{12}$ so $\Delta EI/EI = (1-d/h)^3 - 1$ with h the height of the beam.

Table 8
Function $G_n(x_m)$ for a notch of depth d (1–6 mm) at x_0=0.225 m and with n=1 to 7 frequencies used.

n	$G_n(x_0)$	$G_n(x_m^1)$	$G_n(x_m^2)$	$G_n(x_m^3)$	$G_n(x_m^4)$	$G_n(x_m^5)$	$G_n(x_m^6)$
1	0.156	0.163	0.163	0.152	0.158	0.158	0.174
2	0.633	0.653	0.653	0.622	0.637	0.637	0.683
3	1.096	1.107	1.107	1.089	1.099	1.099	1.122
4	1.014	0.989	0.989	1.028	1.009	1.009	0.944
5	0.438	0.393	0.393	0.466	0.429	0.429	0.323
6	0.013	0.004	0.004	0.021	0.011	0.011	$4 \cdot 10^{-4}$
7	0.214	0.265	0.265	0.186	0.224	0.224	0.352

Table 9
Relative variations of the bending stiffness $\frac{\Delta EI \Delta L}{EIL}$ for a notch of depth d (1–6 mm).

d (mm)	1	2	3	4	5	6
p=1 to 3	−0.0006	−0.0022	−0.0057	−0.0147	−0.0297	−0.0630
p=1 to 4	−0.0006	−0.0022	−0.0055	−0.0144	−0.0278	−0.0600
p=1 to 5	−0.0005	−0.0022	−0.0053	−0.0141	−0.0272	−0.0597
p=1 to 6	−0.0005	−0.0022	−0.0053	−0.0141	−0.0272	−0.0597
p=1 to 7	−0.0005	−0.0021	−0.0053	−0.0141	−0.0271	−0.0585
p=1 to 5 and 7	**−0.0005**	**−0.0021**	**−0.0053**	**−0.0141**	**−0.0271**	**−0.0585**
p=2 to 5 and 7	−0.0006	−0.0021	−0.0053	−0.0141	−0.0272	−0.0585
p=3 to 5 and 7	−0.0005	−0.0020	−0.0052	−0.0139	−0.0268	−0.0568

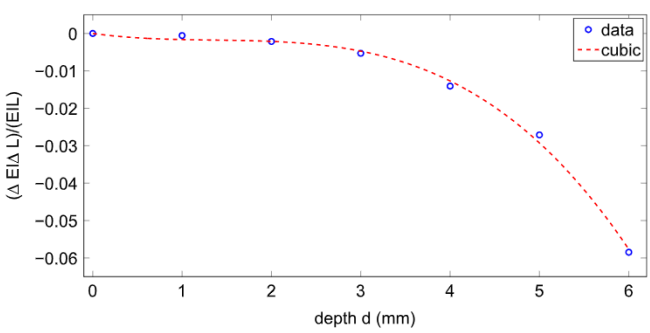

Fig. 7. Relative variations of the bending stiffness $\frac{\Delta EI \Delta L}{EIL}$ depending on the notch depth d. Its third order polynomial approximation, with $\frac{\Delta EI \Delta L}{EIL}(0)=0$, is given by $\frac{\Delta EI \Delta L}{EIL}(d) = -5 \cdot 10^{-4} d^3 + 2.2 \cdot 10^{-3} d^2 - 3.3 \cdot 10^{-3} d$.

Denoting by $Q_p^d(x)$ the function corresponding to the depth d and using p frequencies, we can first verify in Fig. 8 that the variation in the normalized function $\widehat{Q}_p^d(x)$ depends only on the localization x_0 and on the type of the crack, but not on its depth d. Due to the boundary conditions, these functions are equal to zero at both ends. For $p \geq 4$, the minima on the open interval $]0, L[$ for a modification located at x_0, are observed at x_m and at the symmetric value $L - x_m$. The same result is obtained even for small depths.

The second and most important remark is that the norms $\| Q_p^d \|_\infty$ vary regularly with the depth of the notch (d=1–6 mm) and with the number of considered modes (p=1–7) as shown in Fig. 9. The small difference between the curves for p=5 and p=6 is due to the fact that the frequency relative variation for the sixth mode is close to zero (Table 5). Indeed the modification location (x_0=0.225 m) is close to a vibration node of the sixth mode (x=0.230 m).

It is important to note that the norm $\| Q_p^d \|_\infty$ is a useful indicator as it can quantify the modification even if the localization procedure fails. The evolution of the norm, that increases according to the modification, is not dependent of the modification location.

4.2.2. Influence of the position of a stiffness modification in case of a cantilever beam

To study the influence of the modification position on its accuracy, our procedure was applied here to an aluminum cantilever beam studied by Agarwalla [25]. These authors studied an aluminum cantilever beam of length L=0.8 m, width b=0.05 m, and height h=0.006 m with a notch of constant depth (3 mm) and varying notch locations: x_0=0.2 m, 0.4 m, and 0.6 m from the clamped end. The first three measured natural frequencies given in Table 10 are in good agreement with those numerically calculated.

Using these three measured natural frequencies, the $Q_3(x)$ function was computed for each notch location. As seen in previous examples, the localization of the notch is more obvious when the normalized function $\widehat{Q}_3(x) = \frac{Q_3(x)}{\| Q_3 \|_\infty}$ is plotted..

In Fig. 10, it can be noted that when x_0=0.2 m, x_m=0.21 m and $\widehat{Q}_3(x_m) = 0.02$, whereas when x_0=0.4 m, x_m=0.37 m and $\widehat{Q}_3(x_m) = 0.06$. The estimated location x_m is less accurate for x_0=0.4 m than for x_0=0.2 m, which is indicated by the less sharp minimum for x_0=0.4 m. For x_0 = 0.6 m, there is no local minimum but only a small change in the slope of the curve, due to the fact that $\widehat{Q}_3(x)$ is close to zero when x is close to L.

Since the relative variation of the nth frequency is proportional to $G_n(x_0)$ and that $G_1(x)$ is very close to zero when x is close to L, in the case of a modification near the free end of the beam, the first frequency is removed in Eq. (28) and a new function $Q_{2-p}(x)$ is

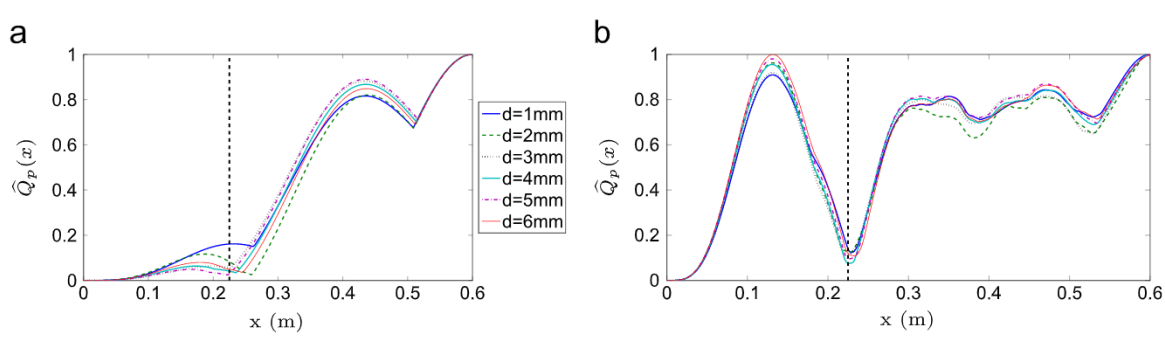

Fig. 8. Normalized function $\widehat{Q}_p(x)$ ($=Q_p(x)/\| Q_p \|_\infty$) for a notch at x_0=0.225 m and different depths (1–6 mm) with (a) p=3 and (b) p=7 frequencies used. Vertical dotted line indicates the location of the notch. The localization of the modification is much better when more frequencies are used and the shape of the function is not depending on the level of the modification.

proposed:

$$Q_{2-p}(x) = \min_{x \in [0,L]} \sum_{2 \le m < n \le p} |F_{m,n}(x)| . \tag{36}$$

As $p=3$ here, only the second and the third modes are taken into account and the function $\widehat{Q}_{2-3}(x)$ is plotted in Fig. 11(a). This function presents a minimum at $x_m=0.638$ m, close to the real position of the modification at $x_0=0.6$ m. Two other minima appear near $x=0.2$ m but these positions can be rejected because they are not significant minima of the function $\widehat{Q}_3(x)$ depending on the three modes. In Fig. 11(b), the normalized function $\widehat{Q}_p(x)$, obtained by numerical simulations of the cantilever beam in order to access more frequencies, is depicted for $p=3$ to 5.

In conclusion, when the notch is far from the free end, three frequencies are enough to localize the notch. However, when the notch is close to the free end, it is recommended to use the additional information given by $\widehat{Q}_{2-p}(x)$ when the contribution of the first mode is omitted (more details can be found in [28]) or to use more frequencies when possible (Fig. 11(b)).

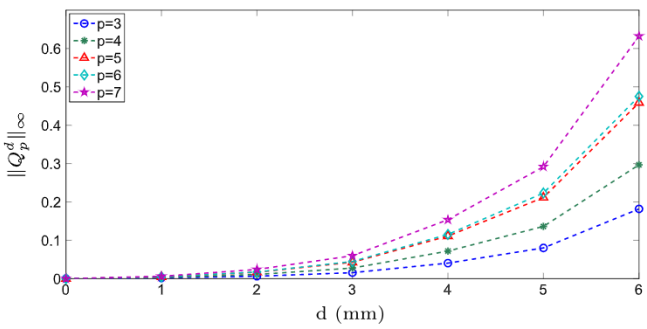

Fig. 9. Graphs of $\|Q_p^d\|_\infty$ for different frequencies used ($p=3$–7) and different depths of the notch ($d=1$–6 mm). The norm of the function increases with the level of the modification and also with the number of frequencies used. The curves for $p=5$ and $p=6$ are close because the frequency relative variation for the sixth mode is near to zero (Table 5).

Table 10
Experimental frequencies (in Hz) and frequency relative variations (in parentheses, in %) for a cantilever beam with notch at 0.2 m, 0.4 m, and 0.6 m from the clamped end (total length of the beam $L=0.8$ m). Taken from Agarwalla [25].

f_n	Healthy	$x_0=0.2$ m	$x_0=0.4$ m	$x_0=0.6$ m
f_1	7.48	7.39 (−1.26)	7.42 (−0.85)	7.47 (−0.21)
f_2	46.63	46.57 (−0.14)	45.87 (−1.64)	46.40 (−0.50)
f_3	130.98	129.51 (−1.12)	130.85 (−0.10)	128.41 (−1.96)

5. Conclusion

This paper discusses the development of a procedure for localization and quantification of modifications using the transverse vibrations of an Euler–Bernoulli beam with or without axial force. Two states are considered: an initial or "healthy" one and a modified or "damaged" one with simultaneous modifications which can concern axial force, mass density and/or bending stiffness. The first natural frequencies, the corresponding mode shapes and first two mode shape derivatives of the initial state, plus the first natural frequencies of the modified state are assumed to be known. The knowledge of the mode shapes of the modified beam is thus not needed.

Expanding the variation of the eigenvectors in the basis of the eigenvectors of the unmodified state, a first-order relation has been first established from the continuous formulation for each mode. This relation links the different relative variations of natural frequency, axial force, bending stiffness, and mass density. When internal modifications of a beam (bending stiffness and/or mass density) are localized, this relation allowed us to build a localization and quantification procedure of these modifications. The proposed procedure gives first an estimation of the localization of the modification using the mode shapes of the initial state and then an estimation of the relative variations of axial force and/or

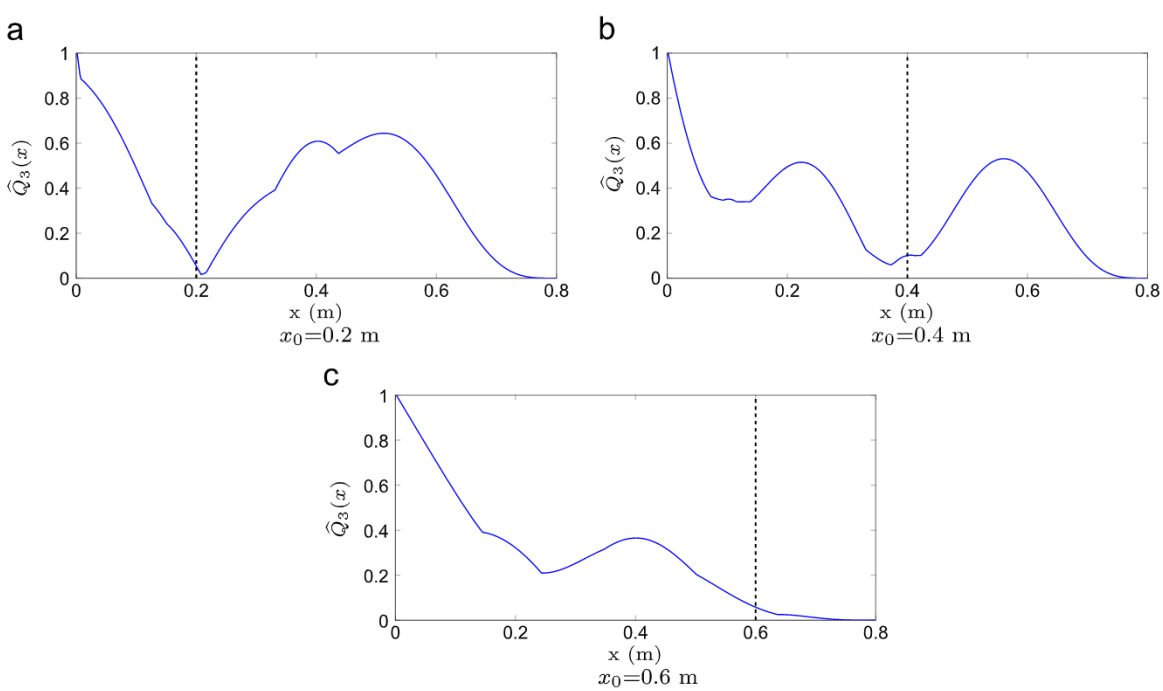

Fig. 10. Normalized function $\widehat{Q}_3(x)$ for a cantilever beam of length 0.8 m and different notch locations: (a) 0.2 m, (b) 0.4 m, and (c) 0.6 m. Vertical dotted line indicates the location of the notch. The localization of the modification is accurate enough for notch location at $x_0=0.2$ m and 0.4 m. When the modification location is near the free edge of the beam, the procedure is not as effective.

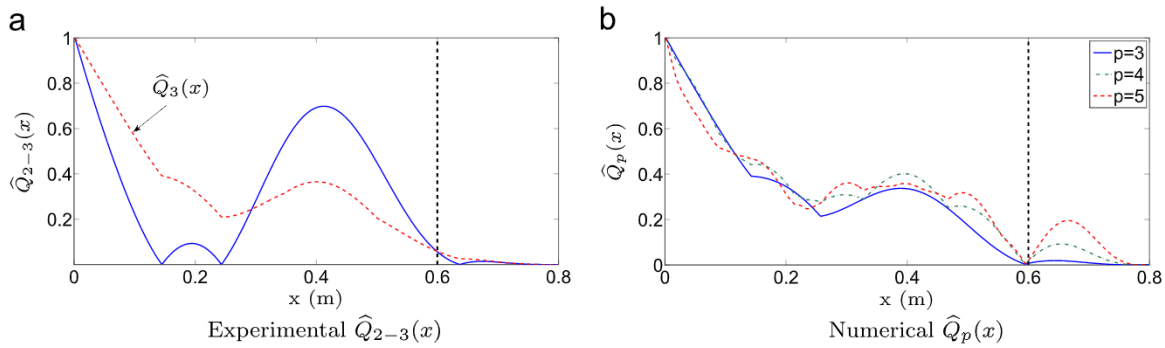

Fig. 11. Normalized function (a) $\widehat{Q}_{2-3}(x)=Q_{2-3}(x)/\|Q_{2-3}\|_\infty$ with $Q_{2-3}(x)=|F_{2,3}(x)|$ and (b) $\widehat{Q}_p(x)$ with $p=3$ to 5 for a cantilever beam of length 0.8 m and a notch located at $x_0=0.6$ m. Vertical dotted line indicates the location of the notch. By omitting the first mode in the normalized function (a), the localization procedure is improved. This is also the case for the numerical simulation of the procedure for the cantilever beam with more frequencies used (b). The location of the notch obtained with numerical frequencies (Fig. 11(b)) is more accurate than that obtained with the experimental frequencies (Fig. 11(a)) due to the effect of noise within the experiments.

mass density and/or bending stiffness through a linear optimization technique.

It has been first applied on numerical finite element simulations, when simultaneous modifications of axial force, density, and bending stiffness are present. The results of both the localization and the quantification of the modification are very satisfactory.

For experimental validations, the localization procedure has been successfully used on real data obtained from beams without axial force. Two cases are presented: a localized change of mass on a clamped–clamped beam and a notch on free–free and cantilever beams, respectively. For the first case, the proposed method was able to localize and to quantify two low modifications of mass with a good accuracy, both on spatial localization and quantification of the mass change. For the free–free beam with a notch, it provided better estimates of the modification location compared to similar techniques in literature. Our procedure takes advantage of the variation of more frequencies. We have also shown that the infinity norm of the function introduced in the procedure is correlated to the magnitude of the internal modification and thus can be used to detect and quantify the modification. When the notch is close to the free end of a cantilever beam, the modification is more difficult to localize. We proposed a method to overcome this difficulty and improve the efficiency of the localization procedure.

At last, new experiments are being set up to further test the validity of our procedure and, if necessary to improve its reliability in more complex situations.

Appendix A

Eq. (17) minus Eq. (5) is zero for any $u(x)\in H^2(0,L)$ within the boundary conditions. The left-hand side can be decomposed as the sum of two terms: the first term $A_n(u)$ containing $\Delta\phi_n(x)$ and the second term $B_n(u)$ containing all the other first-order terms $\Delta EI(x)$, ΔT, $\Delta\mu(x)$, and $\Delta\lambda_n$. Hence, choosing $u(x)=\phi_n(x)$ and taking into account Eq. (6), the orthogonality of the normal modes with respect to the mass density and Eq. (10), the terms with $k\neq n$, cancel and the first term $A_n(u)$ can be written as

$$A_n(\phi_n)=\int_0^L\left(EI(x)\Delta\phi_n''(x)\phi_n''(x)+T\Delta\phi_n'(x)\phi_n'(x)-\lambda_n\mu(x)\Delta\phi_n(x)\phi_n(x)\right)$$

$$\mathrm{d}x=\alpha_{nn}\int_0^L\left(EI(x)\phi_n''^2(x)+T\phi_n'^2(x)-\lambda_n\mu(x)\phi_n^2(x)\right)\mathrm{d}x \tag{A.1}$$

The integral is equal to zero due to Eq. (7). When $u(x)=\phi_n(x)$, the second term $B_n(u)$ becomes

$$B_n(\phi_n)=\int_0^L\left(\Delta EI(x)\phi_n''^2(x)+\Delta T\phi_n'^2(x)\,\mathrm{d}x-\Delta\lambda_n\mu(x)\phi_n^2(x)-\lambda_n\Delta\mu(x)\phi_n^2(x)\right)\mathrm{d}x \tag{A.2}$$

Since $A_n(\phi_n)+B_n(\phi_n)=0$ and $A_n(\phi_n)$ is null, the expression above is equal to zero. This yields the following first-order estimate of the variation in the eigenvalue:

$$\Delta\lambda_n\int_0^L\mu(x)\phi_n^2(x)\,\mathrm{d}x\approx\int_0^L\Delta EI(x)\phi_n''^2(x)\,\mathrm{d}x+\Delta T\int_0^L\phi_n'^2(x)\,\mathrm{d}x-\lambda_n\int_0^L\Delta\mu(x)\phi_n^2(x)\,\mathrm{d}x \tag{A.3}$$

The first-order estimate of Eq. (A.3) can be modified using Eq. (9) to express the λ_n relative variation as a linear function of the relative structural modification (e.g. Eq. (20)).

References

[1] Gobbato M, Conte JP, Kosmatka JB, Farrar CR. A reliability-based framework for fatigue damage prognosis of composite aircraft structures. Probab Eng Mech 2012;29:176–88.
[2] Lei Y, Lin J, He Z, Zuo MJ. A review on empirical mode decomposition in fault diagnosis of rotating machinery. Mech Syst Signal Process 2013;35(1–2):108–26.
[3] Sposito G, Ward C, Cawley P, Nagy PB, Scruby C. A review of non-destructive techniques for the detection of creep damage in power plant steels. NDT & E Int 2010;43(7):555–67.
[4] Salawu OS. Detection of structural damage through changes in frequency: a review. Eng Struct 1997;19(9):718–23.
[5] Doebling SW, Farrar CR, Prime MB. A summary review of vibration-based damage identification methods. Shock Vib Digest 1998;30:91–105.
[6] Sinou J-J. A review of damage detection and health monitoring of mechanical systems from changes in the measurement of linear and non-linear vibrations. Mech Vib: Meas Effects Control 2009:643–702.
[7] Fan W, Qiao P. Vibration-based damage identification methods: a review and comparative study. Struct Health Monit 2011;10(1):83–111.
[8] Chesné S, Deraemaeker A. Damage localization using transmissibility functions: a critical review. Mech Syst Signal Process 2013;38(2):569–84.
[9] Heylen W, Lammens S, Sas P. Modal analysis theory and testing. Leuven, Belgium: Katholieke Universiteit Leuven, Departement Werktuigkunde; 1997.
[10] Maia NMM, Silva JMM. Theoretical and experimental modal analysis. Taunton, UK: Research Studies Press; 1997.
[11] Ewins DJ. Modal testing: theory and practice. Letchworth, UK: Research Studies Press; 1986.
[12] Pandey AK, Biswas M, Samman MM. Damage detection from changes in curvature mode shapes. J Sound Vib 1991;145:321–32.
[13] Cao M, Ye L, Zhou L, Su Z, Bai R. Sensitivity of fundamental mode shape and static deflection for damage identification in cantilever beams. Mech Syst Signal Process 2011;25(2):630–43.
[14] Jassim ZA, Ali NN, Mustapha F, Abdul Jalil NA. A review on the vibration analysis for a damage occurrence of a cantilever beam. Eng Failure Anal 2013;31:442–61.

[15] Lin H-P, Chang S-C. Forced responses of cracked cantilever beams subjected to a concentrated moving load. Int J Mech Sci 2006;48:1456–63.
[16] Attar M. A transfer matrix method for free vibration analysis and crack identification of stepped beams with multiple edge cracks and different boundary conditions. Int J Mech Sci 2012;57:19–33.
[17] Friswell MI, Penny JET. Crack modeling for structural health monitoring. Struct Health Monit 2002;1(2):139–48.
[18] Narkis Y, Elmalah E. Crack identification in a cantilever beam under uncertain end conditions. Int J Mech Sci 1996;38(5):499–507.
[19] Khaji N, Shafiei M, Jalalpour M. Closed-form solutions for crack detection problem of Timoshenko beams with various boundary conditions. Int J Mech Sci 2009;51:667–81.
[20] Bakhtiari-Nejad F, Khorram A, Rezaeian M. Analytical estimation of natural frequencies and modeshapes of a beam having two cracks. Int J Mech Sci 2014;78:193–202.
[21] Morassi A. Damage detection and generalized Fourier coefficients. J Sound Vib 2007;302(1–2):229–59.
[22] Goldfeld Y, Elias D. Using the exact element method and modal frequency changes to identify distributed damage in beams. Eng Struct 2013;51:60–72.
[23] Esfandiari A, Bakhtiari-Nejad F, Rahai A. Theoretical and experimental structural damage diagnosis method using natural frequencies through an improved sensitivity equation. Int J Mech Sci 2013;70:79–89.
[24] Nahvi H, Jabbari M. Crack detection in beams using experimental modal data and finite element model. Int J Mech Sci 2005;47:1477–97.
[25] Agarwalla DK, Parhi DR. Effect of crack on modal parameters of a cantilever beam subjected to vibration. Procedia Eng 2013;51:665–9.
[26] Binici B. Vibration of beams with multiple open cracks subjected to axial force. J Sound Vib 2005;287(1–2):277–95.
[27] Hsu MH. Vibration analysis of edge-cracked beam on elastic foundation with axial loading using the differential quadrature method. Comput Methods Appl Mech Eng 2005;194(1):1–17.
[28] Le TTH. Contribution à la détection, à la localisation d'endommagements par des méthodes d'analyse dynamique des modifications structurales d'une poutre avec tension – Application au suivi des câbles du génie civil [PhD thesis], Ecole Nationale des Ponts et Chaussées; 2014.
[29] Ruocci G, Cumunel G, Le TTH, Argoul P, Point N, Dieng L. Damage assessment of pre-stressed structures: a SVD-based approach to deal with time-varying loading. Mech Syst Signal Process 2014;47(1–2):50–65.
[30] Dilena M, Morassi A. The use of antiresonances for crack detection in beams. J Sound Vib 2004;276(1–2):195–214.
[31] Le TP, Argoul P. Continuous wavelet transform for modal identification using free decay response. J Sound Vib 2004;277:73–100.
[32] Cumunel G, Le TTH, Point N, Argoul P. Detection of structural modifications of an Euler–Bernoulli beam through modal parameters variation. In: EWSHM – 7th European workshop on structural health monitoring, Nantes, France; July 2014.
[33] Argoul P, Le TP. Instantaneous indicators of structural behaviour based on the continuous Cauchy wavelet analysis. Mech Syst Signal Process 2003;17(1):243–50.
[34] Morassi A. Identification of a crack in a rod based on changes in a pair of natural frequencies. J Sound Vib 2001;242(4):577–96.